

Acceleration of Polarized Protons at RHIC¹

Haixin Huang

Collider-Accelerator Department, Brookhaven National Laboratory, Upton, NY 11973, USA

Abstract. Relativistic Heavy Ion Collider (RHIC) ended its second year of operation in January 2002 with five weeks of polarized proton collisions. Polarized protons were successfully injected in both RHIC rings and maintained polarization during acceleration up to 100 GeV per ring using two Siberian snakes in each ring. This is the first time that polarized protons have been accelerated to 100 GeV. The machine performance and accomplishments during the polarized proton run will be reviewed. The plans for the next polarized proton run will be outlined.

INTRODUCTION

The highly successful program of QCD and electroweak tests at the hardron colliders at CERN and FNAL has provided a wealth information on the Standard Model of particle physics. One aspect of our understanding which has not benefited from such experiments at high-energy colliders, however, is the area of spin physics, both spin structure of the proton itself and the spin-dependence of the fundamental interactions.

The RHIC center-of-mass energy range of 200 to 500 GeV is ideal for such studies in the sense that it is high enough for perturbative QCD to be applicable and low enough so that the typical momentum fraction of the valence quarks is about 0.1 or larger. This guarantees significant levels of parton polarizations. RHIC spin program utilizes two Siberian snakes [1] and four spin rotators in each ring to accelerate polarized protons to 250 GeV with 70% polarization. The first polarized proton collider run in RHIC took place from December 2001 to January 2002. Polarized beams were successfully accelerated to 100 GeV. They were stored and collided with a peak luminosity of about $1.5 \times 10^{30} \text{ cm}^{-2} \text{ s}^{-1}$.

SPIN DYNAMICS

In the presence of magnetic fields, the spin is governed by the Thomas-BMT (Bargmann, Michel, and Telegdi) Equation [2],

$$\frac{d\vec{S}}{dt} = \frac{e}{\gamma m} \vec{S} \times \left(G\gamma \vec{B}_{\perp} + (1 + G)\vec{B}_{\parallel} \right), \quad (1)$$

¹ This work was supported by the Department of Energy of United States.

where \vec{S} is the spin vector of a particle in the frame that moves with the particle's velocity, \vec{B}_\perp and \vec{B}_\parallel are defined in the laboratory rest frame with respect to the particle's velocity. $G = \frac{g-2}{2}$ is the gyromagnetic anomaly of the proton, and γ is the Lorentz factor. It is similar to the equation of motion for a particle moving in magnetic fields,

$$\frac{d\vec{v}}{dt} = \frac{e}{\gamma m} \vec{v} \times (\vec{B}_\perp), \quad (2)$$

where \vec{v} is the velocity of the particle. By comparing the two equations, one can see that for a pure vertical field, spin rotates $G\gamma$ times faster than orbital motion. Eq. (1) also shows that the spin precession with a vertical field is independent of energy (γ) while the horizontal field has to linearly increase with energy to obtain the same spin precession. For general spin manipulation, longitudinal fields are used at low energy and transverse fields are used at high energy.

In a perfect planar synchrotron with vertically oriented guiding magnetic field, the spin vector of a proton beam precesses around the vertical axis $G\gamma$ times per orbital revolution. The number of precessions per revolution is called the spin tune ν_{sp} and is equal to $G\gamma$ in this case. In a real circular accelerator, the horizontal magnetic field that arises from various sources, such as the vertical closed orbit and the vertical betatron oscillation, kicks the spin vector away from the precessing around the vertical axis. Normally, this perturbation is small. However, when the spin precession frequency coincides with the frequency at which the spin vector gets kicked by the horizontal magnetic field, the spin vector is kicked away coherently and a spin depolarizing resonance is encountered. The spin resonance strength ε_k is defined as the Fourier amplitude of the spin perturbing field.

In general, a spin resonance is located at

$$\nu_{sp} = G\gamma = k \pm l\nu_y \pm m\nu_x \pm n\nu_{syn}, \quad (3)$$

where k, l, m and n are integers, ν_x and ν_y are horizontal and vertical betatron tunes, and ν_{syn} is the tune of the synchrotron oscillation. There are three main types of depolarizing resonances: imperfection resonances at $\nu_{sp} = k$, intrinsic resonances at $\nu_{sp} = l \pm \nu_y$ and coupling resonances at $\nu_{sp} = n \pm \nu_x$. The imperfection resonance is due to the vertical closed orbit error, and its strength is proportional to the size of the closed orbit distortion. The intrinsic resonance comes from the vertical betatron motion and are determined by the size of the vertical betatron oscillation. The larger the betatron oscillation, the stronger the resonance. The coupling resonance is caused by the vertical motion with horizontal betatron frequency due to linear coupling [3]. The strength of coupling resonance is proportional to the coupling coefficient in addition to the beam emittance. The acceleration of polarized proton beam in RHIC from 25 GeV/c to 250 GeV/c crosses numerous spin resonances. Fig. 1 shows the imperfection and intrinsic spin resonance strength as a function of the beam energy in RHIC. Because the RHIC lattice contains 3 superperiods and 27 effective FODO cells in each superperiod, the imperfection spin resonances at $G\gamma = k \times 81$ and intrinsic spin resonances at $G\gamma = k \times 81 \pm (\nu_y - 12)$ with $k = 3, 5$ are strongly enhanced. The factor $(\nu_y - 12)$ is because there are total 12 insertion regions in RHIC and the phase advance of each insertion region

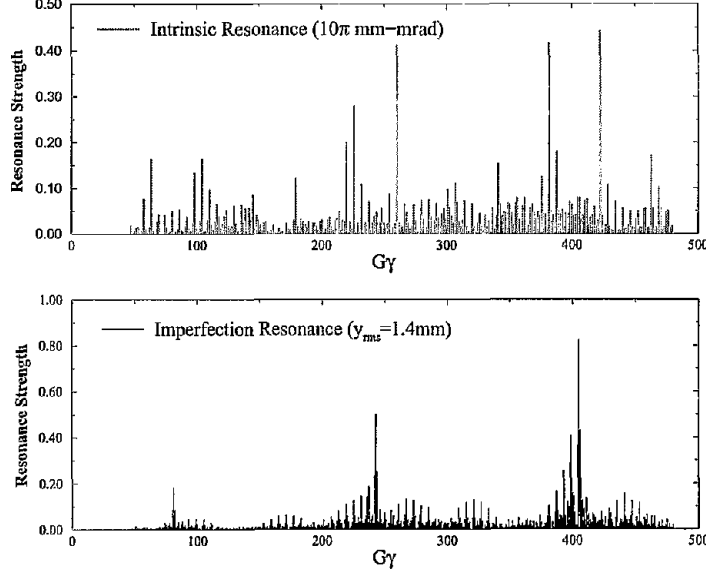


FIGURE 1. RHIC spin resonance spectrum. The top plot is for the intrinsic resonances and the bottom plot is for imperfection resonances. A lattice of RHIC 2000 polarized proton commissioning was used.

is π . The spin resonances with $k = \text{even integers}$ are weakened because arrangement of the focusing and defocusing quadrupoles on either side of each interaction point (IP) is antisymmetric.

When a polarized beam is uniformly accelerated through an isolated spin resonance, the final polarization P_f is related to the initial polarization P_i by the Froissart-Stora formula[4]

$$P_f = (2e^{-\pi|\epsilon_k|^2/2\alpha} - 1)P_i, \quad (4)$$

where α is the rate of change of spin tune per radian of the orbit angle due to acceleration:

$$\alpha = \frac{d(G\gamma)}{d\theta}, \quad (5)$$

and θ is the orbital angle in the synchrotron. In the AGS, a few weak intrinsic resonances were not corrected with any scheme. The final polarization were affected by the value of α .

For a ring with a partial snake with strength s , the spin tune ν_{sp} is given by

$$\cos \pi \nu_{sp} = \cos \frac{s\pi}{2} \cos G\gamma\pi, \quad (6)$$

where $s = 1$ would correspond to a full snake which rotates the spin by 180° . When $s=1$, the spin tune is always $1/2$ and energy independent. Thus, all imperfection, intrinsic

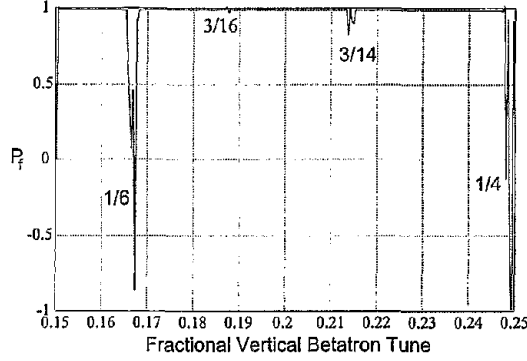


FIGURE 2. Vertical polarization after acceleration through a strong intrinsic resonance and a moderate imperfection resonance shown as a function of the vertical betatron tune.

sic and coupling resonance conditions can be avoided. However, when the spin resonance strength is large, a new class of spin-depolarizing resonance can occur. These resonances, due to coherent higher-order spin-perturbing kicks, are called snake resonances [5] and located at

$$\Delta v_y = \frac{k \pm v_{sp}}{n}, \quad (7)$$

where Δv_y is the fractional part of vertical betatron tune, n and k are integers, and n is called the Snake resonance order. Fig. 2 shows the result of a simple spin tracking through an energy region (using RHIC ramp rate) with an intrinsic resonance strength of 0.5 and an imperfection resonance strength of 0.05. There are clearly regions of the betatron tunes that should be avoided. It should be noted that when coupling is present, Eq. (7) also applies to horizontal tune v_x .

POLARIZED PROTONS IN RHIC INJECTOR

The Brookhaven polarized proton facility complex is shown schematically in Fig.3. The polarized H^- beam from the optically pumped polarized ion source (OPPIS) [6] was accelerated through a radio frequency quadrupole and the 200 MeV LINAC. The OPPIS source produced 10^{12} polarized protons per pulse. The beam polarization at 200 MeV was measured with elastic scattering from a carbon fiber target. During the run, the polarization measured by the 200 MeV polarimeter was about 70%. The beam was then strip-injected and accelerated in the AGS Booster up to 2.5 GeV or $G\gamma = 4.7$. The vertical betatron tune of the AGS Booster was chosen to be 4.9 in order to avoid crossing the intrinsic resonance $G\gamma = 0 + v_y$ in the Booster. The imperfection resonances at $G\gamma = 3, 4$ were corrected by harmonic orbit correctors.

Only one of the twelve rf buckets in the AGS was filled, and the beam intensity varied between $1.3 - 1.7 \times 10^{11}$ protons per fill. At the AGS, a 5% partial Siberian snake [7] that rotates the spin by 9° is sufficient to avoid depolarization from imperfection resonances up to the required RHIC transfer energy [8]. Full spin flip at the four strong intrinsic

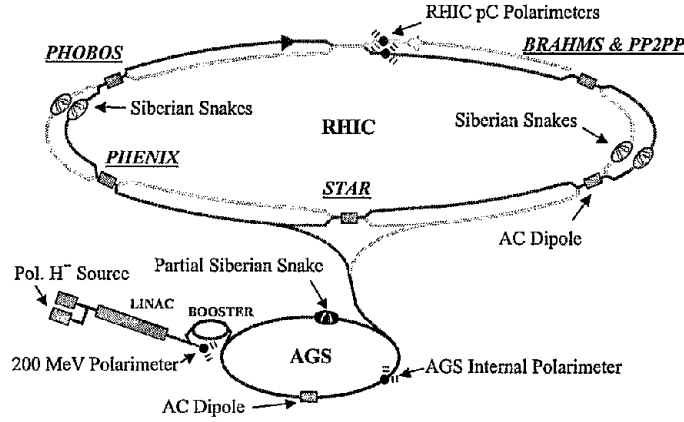


FIGURE 3. The Brookhaven polarized proton facility complex, which includes the OPPIS source, 200 MeV LINAC, the AGS Booster, the AGS, and RHIC. The clockwise ring is called Blue ring and the counter-clockwise ring is called Yellow ring. There are six IPs in RHIC. Two large detectors, STAR and PHENIX reside at six and eight o'clock IP, respectively. Two polarimeters are installed at straight section in 12 o'clock region. Two snakes are installed at three and nine o'clock sections in each ring.

resonances can be achieved with a strong artificial rf spin resonance excited coherently for the whole beam by firing an ac dipole [9]. The remaining polarization loss in the AGS is caused by coupling resonances and weak resonances. The polarized proton beam was accelerated up to $G\gamma = 46.5$ or 24.3 GeV. The normal main magnet ramp rate gives $\alpha = 4.8 \times 10^{-5}$. The ramp rate was much slower in last run which gave $\alpha = 2.4 \times 10^{-5}$, due to the fact that a back-up AGS main magnet power supply had to be used. This reduced the polarization level at the AGS extraction energy from 40% achieved before down to $\sim 25\%$. Faster acceleration and a future, much stronger partial snake should eliminate depolarization in the AGS [10].

POLARIZED PROTONS IN RHIC

The basic construction unit for RHIC snake is a superconducting helical magnet producing a 4T dipole field that rotates through 360° in a length of 2.4 meters. These magnets are assembled in group of four to build four Siberian snakes (two for each ring) for RHIC [11] [12]. The 9 cm diameter bore of the helical magnets can accommodate 3 cm orbit excursions at injection. Fig. 4 shows the orbit and spin trajectory through a RHIC snake. The superconducting helical dipoles were constructed at BNL using thin cable placed into helical grooves that have been milled into a thick-walled aluminum cylinder. With two snakes in each ring, the stable spin direction is vertical in RHIC and independent of beam energy.

The first RHIC polarized proton run lasted eight weeks, including commissioning and physics running. 60 bunches pattern was used in each ring (55 filled, 5 empty for an abort gap). Different alternating spin bit pattern were used for two rings to provide

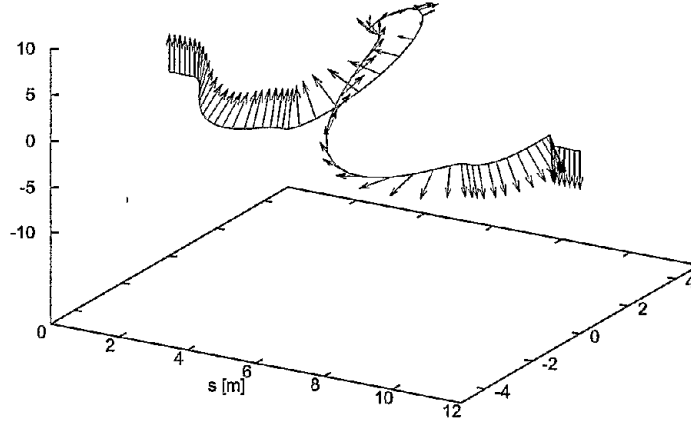


FIGURE 4. Orbit and spin tracking through the RHIC helical snake at $\gamma = 25$. The two axes without label are in the unit of centimeter. The spin tracking shows the reversal of the vertical polarization.

four different spin collision combinations. Specifically, the spin pattern for Blue ring is $\uparrow\downarrow\downarrow \dots EEEEE$, and the spin pattern for Yellow ring is $\uparrow\uparrow\downarrow \dots EEEEE$, where E means empty bunch. For the last six days, three unpolarized bunches were put into patterns at every twenty bunches. They were useful for bunch-by-bunch polarization study. The beam was injected into RHIC with 3 meter β^* lattice and accelerated up to 100 GeV without beta-squeeze. The total intensity of 4×10^{12} was reached. The typical beam emittance is 25π mm-mrad in both transverse planes.

The fractional betatron tune space ranged between 0.20 and 0.225 for the horizontal tune and between 0.225 to 0.25 for the vertical. The vertical betatron tune was chosen to avoid 3/14 snake resonance (see Fig. 2). During the run it was found that when coupling was strong, the coupling snake resonance could also cause polarization loss. One indication of the strong coupling is shown in Fig. 5.

In RHIC the primary source of coupling comes from quadrupole rolls in the triplet quadrupoles at the six interaction regions. In addition, a small longitudinal field is introduced by each helical dipole snake. Much effort was devoted to compensate the rolls in the triplet quadrupoles through a system of local and global corrections outlined in Ref. [13]. These efforts produced some success at injection and flattop. However, problems during the acceleration ramp persisted since a dynamic correction technique has yet to be implemented. The problem of coupling was further enhanced since the fractional tune space during operation left little distance between the horizontal and vertical tunes. Spin tracking results in the Blue ring using the program SPINK [14] and including rolls in the triplet quadrupoles (without correction) show clearly the onset of the coupled snake resonances as the horizontal tune crosses the 3/14 snake resonance location in Fig. 6. In later RHIC fills, the horizontal betatron tune was moved away from the coupling snake resonance and polarization is preserved through the ramp.

Close attention was also paid to the orbit. The imperfection resonance strength is proportional to the rms orbit error. Fig. 7 shows an orbit history in the ramp for fill 2244.

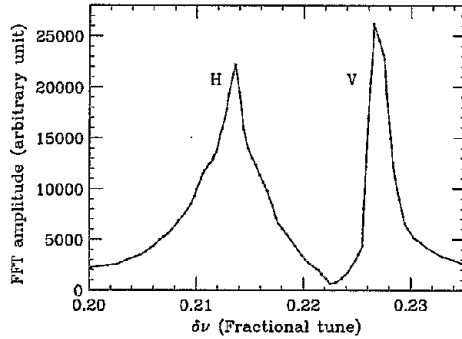


FIGURE 5. Snapshot of the FFT spectrum from the RHIC tune measurement along the ramp in the Yellow ring. For this particular ramp, the polarization preservation efficiency dropped to 20%. This snapshot was taken when crossing one strong resonance location ($G\gamma \sim 100$) along the RHIC ramp with the tunemeter kicker fired only in one plane. The double peak is the clear evidence of strong coupling, where the horizontal tune (lower peak) is clearly overlapping the 3/14 snake resonance.

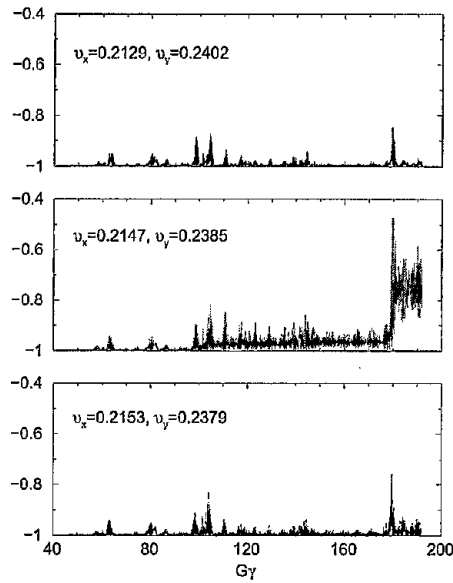


FIGURE 6. Spin tracking results for strongly coupled Blue ring with an emittance of 25π mm-mrad and $\nu_{rms} = 0.6$ mm. The three plots show polarization versus $G\gamma$ with the fractional part of horizontal betatron tune near 3/14. The middle plot shows depolarization due to the coupling snake resonance at 3/14.

In this fill, both rms orbit errors for vertical and horizontal orbits were under 1 mm.

Polarization was measured in RHIC at injection and store with RHIC polarimeters (one in each ring). The details of the polarimeters are given in Ref. [15]. Due to the 5% partial snake in the AGS and several vertical bends in the AGS to RHIC transfer

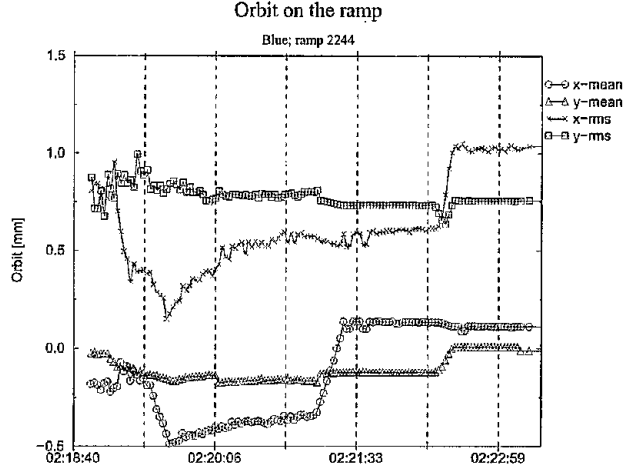


FIGURE 7. RHIC orbit in Blue ring for fill 2244 vs time in the ramp.

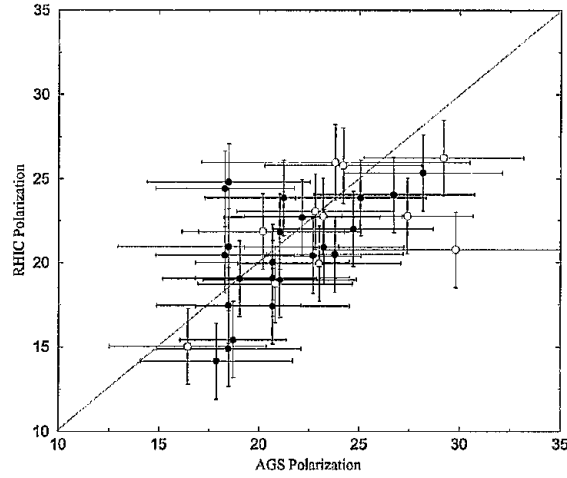


FIGURE 8. Comparison of polarization measured at the AGS polarimeter (at $G\gamma = 46.5$) and the RHIC injection for part of the run. The diagonal line is plotted for a ratio of one. The filled (open) dots are polarization measured at Blue (Yellow) ring injection.

line, the spin transmission efficiency of AGS to RHIC transfer line is less than 100% at $G\gamma = 46.5$ [16]. Nevertheless, the polarization measured at the RHIC injection tracked the AGS polarimeter measurement (at $G\gamma = 46.5$) as shown in Fig. 8. There were about 1000 polarization measurements over the eight weeks running time. With 55 bunches and total intensity of 3.5×10^{12} per ring, the measuring time was about 40 seconds at store to get 20 million events. Since beam intensities were higher at injection, the

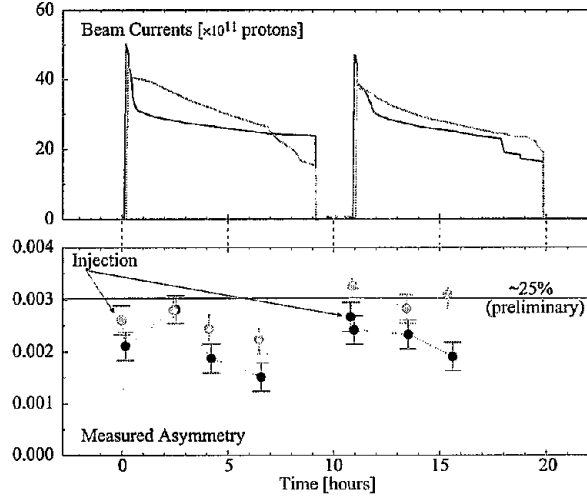


FIGURE 9. Beam intensity and measured asymmetry in the Blue and Yellow rings for two typical stores. The solid curves in the top plot are the beam intensities and the solid dots in the bottom plot are physics asymmetries. Dark (light) lines and symbols are for Blue (Yellow) ring. The asymmetries stayed as constant statistically.

measuring time was about the same. Although the analyzing power at 100 GeV for the RHIC polarimeter is unknown, it is expected to be similar at injection energy. Under this assumption the polarization measured at store was typically about 20-25%. One example is shown in Fig.9.

In summary, to preserve polarization in RHIC, the resonance strengths should be kept lower enough that the two snakes can overcome. A smaller vertical emittance is preferred and vertical orbit error should be as small as possible. The betatron tunes should be carefully set in the good tune window and monitored along the ramp and at store. In addition, attention should be paid to the coupling correction.

OUTLOOK

Spin Rotators are required at the IPs used by PHENIX and STAR to allow measurements of spin effects with longitudinally polarized protons. The spin rotators rotate the polarization from the vertical direction into the horizontal plane on one side of the IP and restore it to the vertical direction on the other side. Eight spin rotators have been installed in the RHIC after last run. They will be commissioned in next run.

Because the same bunches collide for a given experiment, periodically reversing the spin will reduce systematic errors for asymmetry measurements even further. A full spin flip can be induced by slowly sweeping the ac dipole frequency across the spin precession frequency. To achieve this, the spin precession tune needs to be tuned away from its nominal value 0.5. This can be achieved by adjusting the helical snakes' axis

angles. The polarization reversal will take about a few seconds. A brief test has been done during last run and the results are very promising [17]. Same technique will also be used to determine how well the two snake axes are set.

A new vertical survey was done after the run and it revealed that the vertical distortion of magnets in the 12 o'clock area is in the order of several millimeters. Such a big misalignment increases the imperfection resonance strength significantly. It is our high priority to restore the alignment of dipole magnets and it will be done before next run.

The real time tune control system has been tested successfully last run for a few RHIC fills along the up ramp [18]. It is essential to have the tune control system operational next run to control betatron tunes along the ramp. Moreover, the system is crucial for down ramp to decelerate beam back to injection energy.

To calibrate the analyzing power of RHIC polarimeters at any energy above injection, the polarized hydrogen jet target will be needed but it will not be ready until 2004 [19]. An alternative way is to ramp down the energy and measure the asymmetry again at injection. If the asymmetry after down ramp is similar to the measurement before the up ramp, polarization is preserved. The analyzing power at storage energy can then be extracted from the asymmetries measured at injection and store.

Recently, an 11.4% partial Siberian snake was used to successfully accelerate polarized protons through a strong intrinsic depolarizing spin resonance at $0 + \nu_y$ in the AGS [10]. No noticeable depolarization due to $0 + \nu_y$ was observed. This opens up the possibility of using a 20% partial Siberian snake in the AGS to overcome all weak and strong intrinsic spin resonances. With a new strong partial snake in the AGS and higher polarization from the source, the desired 70% polarization could be reached at RHIC.

REFERENCES

1. Ya.S. Derbenev and A.M. Kondratenko, Part. Accel. **8**, 115 (1978).
2. L.H. Thomas, Philos. Mag. **3**, 1 (1927); V. Bargmann, L. Michel, and V.L. Telegdi, Phys. Rev. Lett. **2**, 435 (1959).
3. H. Huang, T. Roser, A. Luccio, Proc. of 1997 IEEE PAC, Vancouver, May, 1997, p.2538.
4. M. Froissart and R. Stora, Nucl. Instrum. Meth. **7**, 297(1960).
5. S.Y. Lee and S. Tepikian, Phys. Rev. Lett. **56**, 1635 (1986).
6. A. Zelenski, *et al.*, in *Proceedings of the 9th International Conference on Ion Sources*, Rev. Sci. Inst., Vol.73, No.2, p.888 (2002).
7. T. Roser, in *Proceedings of the 8th International Symposium on High-Energy Spin Physics*, Minneapolis, 1988, AIP Conf. Proc. No 187 (AIP, New York,1989), p.1442.
8. H. Huang, *et al.*, Phys. Rev. Lett. **73**, 2982 (1994).
9. M. Bai, *et al.*, Phys. Rev. Lett. **80**, 4673 (1998).
10. H. Huang, *et al.*, these proceedings.
11. V.I. Ptitsyn and Yu.M. Shatunov, NIM **A398**, (1997)126.
12. E. Willen *et al.*, Proc. of PAC99, New York, 3161(1999).
13. F. Pilat, *et al.*, Proc. of EPAC2002, Paris, p. 1178.
14. A.U.Luccio *Trends in Collider Spin Physics* World Scientific, p. 235 (1997).
15. O. Jinnouchi, *et al.*, these proceedings; I. Alekseev, *et al.*, these proceedings.
16. W. MacKay, private communication.
17. M. Bai, *et al.*, these proceedings.
18. C. Shuletheiss, *et al.*, Proc. of EPAC2002, Paris, p. 2094.
19. A. Bravar, *et al.*, these proceedings.